Commercial-Scale Demonstration of a First-of-a-Kind Enhanced Geothermal System

Jack H. Norbeck[a] and Timothy M. Latimer[a]

[a]Fervo Energy

114 Main St., Ste. 200, Houston, Texas, USA 77002

Corresponding Author: Jack H. Norbeck

Corresponding Author Email: jack@fervoenergy.com

RESEARCH ARTICLE

Commercial-Scale Demonstration of a First-of-a-Kind Enhanced Geothermal System

Received Date
Accepted Date

DOI: 00.0000/xxxxxxxxxx

Jack H. Norbeck[a] and Timothy M. Latimer[a]

Fervo Energy has completed construction of a commercial enhanced geothermal system (EGS) project and has qualified full functionality of the system through production testing at commercially relevant operating conditions. The project site is located in a nearfield setting adjacent to an operating geothermal power station in north-central Nevada and is designed to deliver an uplift in high-temperature geothermal flow rates to increase the power capacity at the facility.

The project involved drilling a first-of-a-kind EGS horizontal doublet well system, consisting of an injection and production well pair within a high-temperature, hard rock geothermal formation. The lithology of the target reservoir is characterized as a mixed metasedimentary and igneous formation, comprised of phyllite, quartzite, diorite, and granodiorite, representative of the geology across the most prospective geothermal areas throughout the western US. The lateral sections of the wells were drilled with 9 7/8" hole size, completed with 7" casing, extended approximately 3,250 ft horizontally, and reached a maximum measured temperature of 376 °F. A modern multistage, plug-and-perforate stimulation treatment design with proppant was used to enhance the permeability of both horizontal wells. A 37-day crossflow production test was performed in April-May 2023, confirming that the EGS wells are connected hydraulically by a highly conductive fracture network. During production testing, the system achieved flow rates of up to 63 L/s, production temperatures of up to 336 °F and a peak power production of 3.5 MW electric power equivalent. Flow profile wireline logs were performed on the horizontal injection well during the crossflow test, validating that the stimulation treatment design resulted in flow allocation along the entire lateral. Production temperature increased continuously throughout the test, indicating that no significant thermal short-circuit pathways were created during stimulation operations.

Based on a review of historic EGS projects, Fervo's horizontal doublet well design is most productive EGS system to-date in terms of flow rate and electric power equivalent. In successfully completing this project, we have demonstrated that no major technical barriers exist to deploying horizontal EGS systems in similar metasedimentary or igneous formations up to temperatures of approximately 400 °F. Numerical reservoir simulation models calibrated with the field data from this project demonstrate a clear innovation pathway to increasing the power capacity up to 8 MW of electric power per production well, meeting or exceeding the performance criteria outlined in Advanced Scenario the National Renewable Energy Laboratory's 2023 Annual Technology Bulletin for geothermal energy.

1 Introduction

Firm, zero-carbon, dispatchable resources are key to unlocking a fully decarbonized electricity sector (Sepulveda et al. 2018). Geothermal power can play that role - as outlined in the Department of Energy's GeoVision Study and EarthShot Initiative, breakthroughs in enhanced geothermal system (EGS) technologies could unlock over 100 GW of clean, firm power in the United States (DOE 2019; Augustine et al. 2022). But in order to contribute a significant fraction of the energy mix, geothermal projects must be deployed with speed and scale that the industry has not yet achieved (Ricks, Norbeck, and Jenkins 2022). Leveraging technology innovations from the unconventional oil and gas industry provides a pathway to unlocking new geologic resources and improving project economics in a way that could enable geothermal developers to mimic the rapid scale-up observed in shale development over the past two decades (Gradl 2018; Latimer and Meier 2017; Norbeck, McClure, and Horne 2018; Shiozawa and McClure 2014).

Horizontal drilling has the potential to improve geothermal project economics significantly by providing greater access to the target reservoir volume, more consistent flow rates, more uniform flow distribution throughout the reservoir volume, and greater to-

[a] Fervo Energy, 114 Main St., Ste. 200, Houston, Texas, USA 77002

tal heat transfer surface area. In addition, horizontal well designs offer many engineering design decisions that can be optimized to improve reservoir performance, including lateral length, offset well spacing, size of the stimulated reservoir volume, and fracture spacing along the wells. Horizontal well designs, stimulation treatment programs, and reservoir management strategies can be tailored for a given geologic resource which enables a broader range of geologies and locations to be developed than is possible with conventional geothermal development.

In field-scale development programs, horizontal drilling can result in a significant reduction in surface land use because multiple wells can be drilled from a single pad location. Drilling many wells from the same pad can enable cascading cost savings opportunities, such as minimizing in-field rig moves, reducing drilling risk by drilling closely spaced vertical well sections, co-locating surface facilities infrastructure, and minimizing pipeline costs. Perhaps most importantly, the advantages of horizontal drilling described here make it possible to replicate the dramatic learning curve cost-reductions that have been observed in the unconventional oil and gas sector over the last two decades. Drilling many wells in a condensed area allows for geologic, technical and experience learning curves to be applied as a development project progresses, improving project economics over time (Latimer and Meier 2017).

In this paper, we present the results from a field-scale EGS project developed by Fervo Energy that was designed to demonstrate the ability to drill, complete, and operate horizontal EGS wells under commercially relevant operating conditions. The project site is located adjacent to the Blue Mountain geothermal power plant in northern Nevada, therefore the project can be classified as a nearfield EGS project (DOE 2019; NREL 2023). The project involved designing and constructing a 3-well drilling program, including two horizontal wells that formed an injection and production doublet system and a deep vertical monitoring well. The drilling and stimulation phase was completed between January 2022 to March 2023, and the well testing phase was completed between April 2023 to May 2023.

1.1 Geologic Setting

The overall stratigraphic framework at Blue Mountain consists of Miocene to present basin-fill deposits overlying Mesozoic phyllite. The phyllite is intruded by multiple phases of igneous dikes and sills interpreted to be Mesozoic and Tertiary in age. The range-front fault on the SW side of the Blue Mountain forms a prominent topographic break. On the NW side of Blue Mountain, silicified fault breccia is locally exposed in isolated outcrops surrounded by alluvium along the westernmost exposures of the surface trace of this fault. The westernmost exposure of this fault zone is silicified, and the silicification was interpreted to be relict. Kinematic data collected from fault surfaces along the western half of the range-front fault indicate dextral-oblique motion.

Based on the map pattern of the faults and kinematic data, the Blue Mountain geothermal system is associated with a displacement transfer zone (Faulds and Hinz 2016). In this structural model, the range-front along the SW side of the range is dextral-

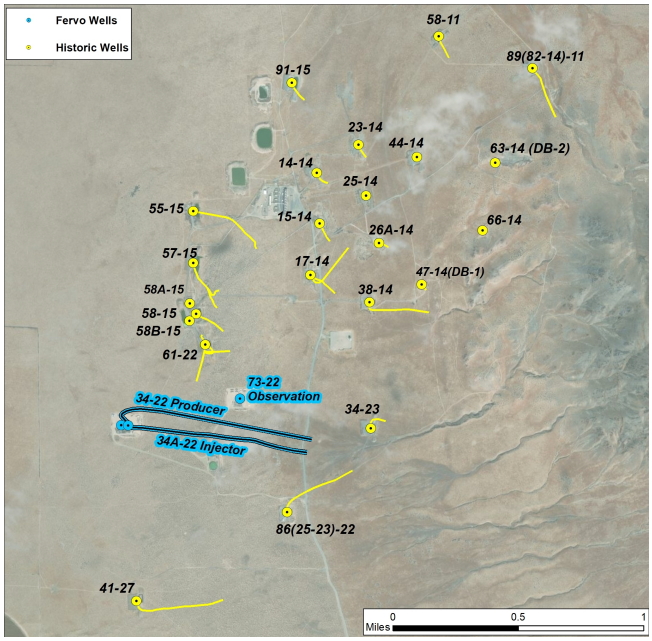

Fig. 1 Site map of the Blue Mountain project area. The Fervo Energy horizontal well EGS doublet system consists of Injection Well 34A-22 and Production Well 34-22, which are located in the southern margin of the field. Monitoring Well 73-22, located at approximately the mid-lateral and to the north of the horizontal doublet system, hosted a permanent fiber optic monitoring system and a downhole gauge to measure reservoir pressure and temperature.

normal. This fault dies out into the basin west of the nose of the range and dextral shear is transferred to NE-striking normal faults that accommodate NW-SE extension in the form of pure dip-slip motion along the NW side of the Blue Mountain range. In this type of model, deep circulation would most likely be controlled by the N to NE-striking normal faults, near where they intersect the NW-striking dextral-normal fault system.

South of the geothermal upflow and outflow zones of the primary hydrothermal system at Blue Mountain, there have been several wells drilled previously (86-22, 41-27, and 34-23) which exhibit relatively conductive temperature conditions and lack deep permeability or connectivity to the rest of the wellfield. This permeability boundary along the south side of the reservoir lies just south of Well 61-22 and has been interpreted to be associated with the down-dip projection of the southwest range-front fault. This recognized lack of deep permeability, reservoir connectivity, and elevated conductive temperatures radiating from the active system to the north makes the southern field relatively compartmentalized, and therefore an ideal testbed for Fervo's horizontal well program. A site map of the project area highlighting the location of the horizontal wells is shown in Fig. 1.

1.2 Horizontal Doublet EGS System Design

A horizontal doublet well system was drilled in the southern margin of the Blue Mountain geothermal field (Injection Well 34A-22 and Production Well 34-22), and a deep vertical monitoring well was also drilled for the purposes of reservoir characterization and stimulation treatment monitoring (Monitoring Well 73-22). The

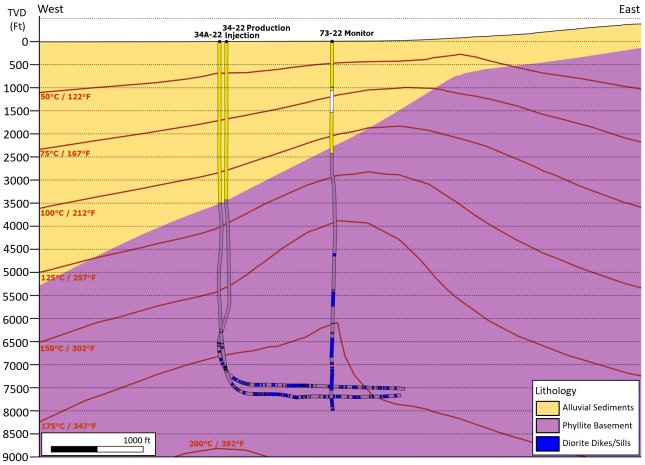

Fig. 2 A cross-section of the horizontal doublet EGS system and deep vertical monitoring well.

horizontal well designs were driven primarily by the following factors: a) the requirement of a 7" production casing string to enable commercial flow rates, b) the requirement of permanent fiber optic cable installation cemented behind the production casing for improved reservoir and wellbore diagnostics, c) a conservative casing program that would be robust against known and unknown geologic hazards in this first of a kind project, d) the local state of stress, and e) the three-dimensional temperature distribution in the reservoir.

The laterals of the two horizontal wells were landed at a true vertical depth of approximately 7,700 ft and the productive lateral sections each extended roughly 3,250 ft. For this first-of-a-kind project, the well construction program was designed conservatively to mitigate known and unknown geologic hazards, including the potential for zones that could cause major fluid losses while drilling. The horizontal wells were designed with four primary casing strings, including a surface casing string set at approximately 800 ft, an intermediate casing string set in the basement formation at approximately 3500 ft, a second intermediate casing string set at the end of the curve at approximately 8000 ft, and the production casing string that ran from surface to the total depth of the well. The production casing was selected as 7", 35 ppf, P-110 casing. Running the production casing string from surface to total depth allowed for permanent fiber optic sensing cables to be installed along both Injection Well 34A-22 and Production Well 34-22. A cross-section of the horizontal wells and monitoring well is shown in Fig. 2.

2 Production Performance of the Fervo System and Comparison to Historic EGS Projects

Upon successfully drilling, completing, and stimulating the horizontal doublet well system, we performed a production test to measure the power capacity of the system as well as to evaluate key performance characteristics of the EGS reservoir. The well test involved circulating geothermal fluid through the doublet system by pumping fluid down Injection Well 34A-22, through the fractured reservoir system, and up Production Well 34-22. Injection pumps located on the well pad and connected to the wellhead of Injection Well 34A-22 provided the pressure to drive fluid through the system; no artificial lift system or downhole production pumps were used. The produced fluid was pumped through a series of holding tanks to provide the residence time for the water to cool sufficiently and was ultimately recirculated for injection. The injectate was a mixture of the produced fluid and saline brine sourced from a nearby groundwater well. Both wells were instrumented to measure wellhead pressure, flow rate, and fluid temperature. Fluid sampling ports we located at several points throughout the system.

The crossflow production test commenced on April 9, 2023 and continued for a 37-day period until May 16, 2023. The test consisted of seven major phases:

1. Constant-rate injection period with the production well shut-in, followed by a 12-hour pressure falloff period
2. Establish crossflow conditions
3. Tracer test
4. Steady-state performance test #1
5. Load-following dispatchability test
6. Wellbore deliverability curve and steady-state performance test #2
7. Wireline flow profile logging and final shut down

Throughout the well test, a valve located just downstream of the Production Well 34-22 wellhead was controlled to maintain backpressure on the system. The wellhead pressure at Production Well 34-22 was maintained at a pressure between approximately 100 psi to 200 psi, which is equivalent to the wellhead pressure anticipated during commercial operations once the system is integrated with the adjacent wellfield and power plant.

2.1 Well Test Results

The electric power of the system can be estimated directly from the field data using the measured flowing thermal power and assuming a thermal-to-electric power conversion efficiency for a relevant power cycle. We anticipate using air-cooled organic Rankine cycle (ORC) technology for Fervo's geothermal power plants. We calculated the equivalent gross electric power production as (Beckers and McCabe 2019):

$$P_{gross} = \eta_u B, \tag{1}$$

where P_{gross} is gross electric power production, η_u is the utilization efficiency of the power plant, and B is the exergy of the produced geothermal fluid. The exergy can be calculated based on the specific enthalpy h and specific entropy s of the geothermal fluid at production (prod) and ambient (0) conditions:

$$B = m_{prod}\left[h_{prod} - h_0 - T_0\left(s_{prod} - s_0\right)\right] \tag{2}$$

where m_{tot} is the mass flow rate of the produced fluid at T_0 is the ambient temperature. beckers2019 provides a methodology

to evaluate the power plant utilization efficiency was evaluated as a function of the produced fluid temperature for a variety of generator technologies.

The electric power required to run the injection pumps can be calculated as:

$$P_{pump} = \frac{q_{inj} p_{inj}}{\eta_{pump}}, \tag{3}$$

where q_{inj} is the volumetric injection rate, p_{inj} is the injection wellhead pressure, and η_{pump} is the pump efficiency, which can be taken directly from the manufacturer's pump curve. For this test, the injection rate and pressure conditions were operated over a sufficiently narrow range to justify assuming a pump efficiency of $\eta_{pump} = 0.80$.

The pumping power acts as a parasitic load on the system, therefore the net electric power generated by the system is:

$$P_{net} = P_{gross} - P_{pump}. \tag{4}$$

Flow rate, pressure, and temperature conditions at Injection Well 34A-22 and Production Well 34-22 were measured continuously throughout the test. Throughout the majority of the test, we were able to ensure that the produced fluid was maintained under single-phase (i.e., liquid) flowing conditions, therefore we do not require any downhole measurements to evaluate the mass flow rate or enthalpy of the produced fluid.

In Figs. 3–5 we show the wellhead pressure, temperature, flow rate, and associated power profiles throughout the full duration of the crossflow test. We observed that the rate and pressure responses between Injection Well 34A-22 and Production Well 34-22 were strongly correlated, with changes in one well causing a rapid response in the offset well typically on the order of minutes to tens of minutes. The rapid response times between the wells validated the most critical technical aspect of the horizontal well EGS system - that the stimulation treatment resulted in a strong hydraulic connection between the wells.

We observed that the system was capable of supporting commercial levels of production. Injection rates throughout most of the test ranged from 650 gpm to 850 gpm, with a maximum injection rate of 1003 gpm. Injection pressures were highly rate-dependent and ranged from 1000 psi to 2000 psi throughout the test. Injection pressures were maintained below the fracturing pressure of approximately 2300 psi. We observed that pressures tended to remain relatively steady while injecting at a constant rate and while actively producing. During periods where the production well was shut-in and we were injecting, injection pressures tended to increase. Injection fluid temperatures ranged from 75 to 125 °F, with the fluctuations being driven by changes in the relative mix of recirculated produced water and makeup water.

Production rates typically ranged from 550 gpm to 750 gpm with a maximum production rate of 970 gpm. Production rates were typically 10 - 20% lower than the injection rates, which can be attributed to leakoff of fluid in the subsurface. The production fluid temperature increased quickly early in the test as the near-wellbore region heated up, and then slowly continued increasing throughout the test to a maximum temperature of 336 °F. Steadily increasing production fluid temperature indicated that the system had no significant fast flowing pathways that could potentially cause premature thermal breakthrough.

A key aspect of the field demonstration was to evaluate the potential to operate the EGS system without the use of artificial lift (e.g., downhole line shaft pump or electrical submersible pump) in the production well. In this circulation test, the pressure to drive flow through the system was provided entirely by a set of horizontal centrifugal pumps connected to the Injection Well 34A-22 wellhead. The wellhead pressure at Production Well 34-22 was controlled by a gate valve located immediately downstream of the wellhead master valve. The producer wellhead was closed for the first 2 days of the test while injection occurred at a constant rate, which allowed the reservoir to pressurize to at least 900 psi above the initial reservoir pressure. At this point, the producer wellhead was opened and the main production phase began. Production flow was sustained entirely by the artificial overpressure conditions in the reservoir. This behavior continued throughout the duration of the crossflow test, which confirms that the system behaved as a relatively confined system and that artificial lift is not required for commercial production.

We used 1 to evaluate the equivalent gross electric power output of the system. We assumed a supercritical ORC power cycle and the ambient temperature was taken as $T_0 = 8$ °C. Gross power output ranged between 2 to 3.5 MW throughout the test. The pumping power requirements ranged from about 500 kW to 1000 kW depending on the injection rate and pressure.

2.2 Comparison to Historic EGS Projects

The first field-scale demonstration of EGS technology was the Fenton Hill project in New Mexico (Brown et al. 2012). Since then, many EGS projects have been developed throughout the world. These projects have tested various stimulation techniques and have taken place in in a wide range of lithologies (Breede et al. 2013; McClure and Horne 2014).

The majority of historic EGS projects can be classified as research and development projects, however, several projects have resulted in commercial production. Most notably, several projects located in the Rhine Graben region on the border of Germany and France are considered commercial EGS projects, including Soultz-sous-Forets and Landau (**blocker2015**; Schindler, Baumgartner, and Gandy 2010). In addition, the Desert Peak EGS project in Nevada resulted in improved injectivity in one well that increased power generation at the facility (Akerley, Robertson-Tait, and Zemach 2020). In both the Rhine Graben and Desert Peak EGS projects, the target formations are considered highly faulted known hydrothermal systems, and circulation was achieved through a combination of stimulated and unstimulated wellbores.

In Fig. 6, we show a comparison of the flow rate from injection, production, or circulation tests performed following the stimulation treatment phase at several of the most well characterized EGS projects against the peak flow rates measured in Injection Well 34A-22 and Production Well 34-22 during our 37-day crossflow test. These results demonstrate that the horizontal well de-

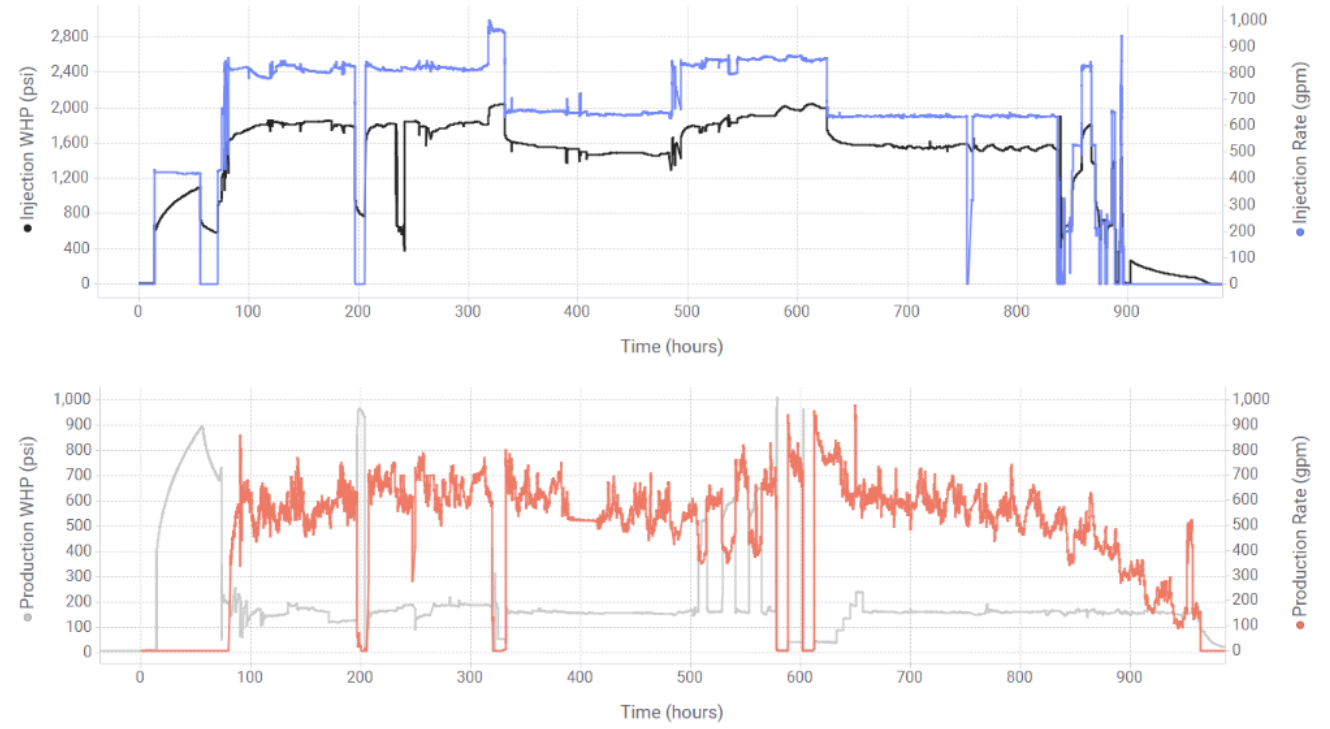

Fig. 3 Flow rate and wellhead pressure recordings during the 37-day circulation test for Injection Well 34A-22 (top) and Production Well 34-22 (bottom).

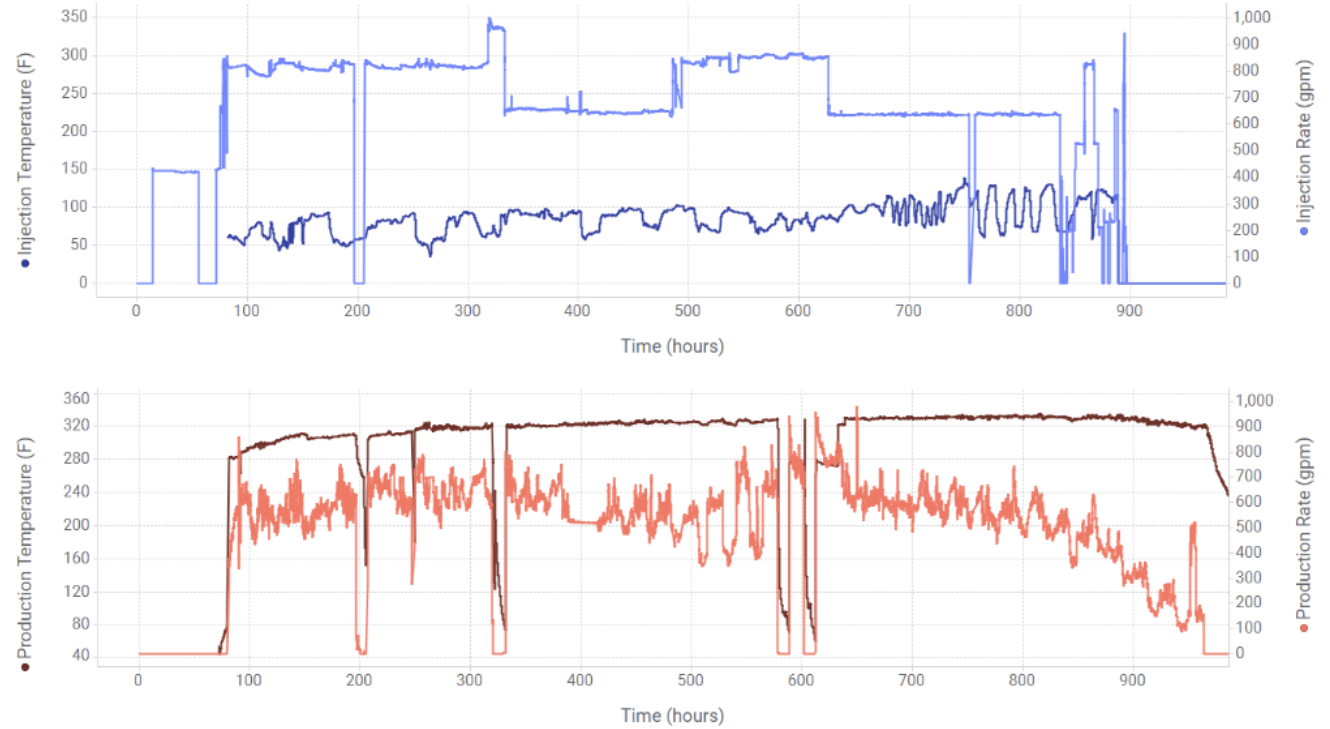

Fig. 4 Flow rate and flowing wellhead temperature recordings during the 37-day circulation test for Injection Well 34A-22 (top) and Production Well 34-22 (bottom).

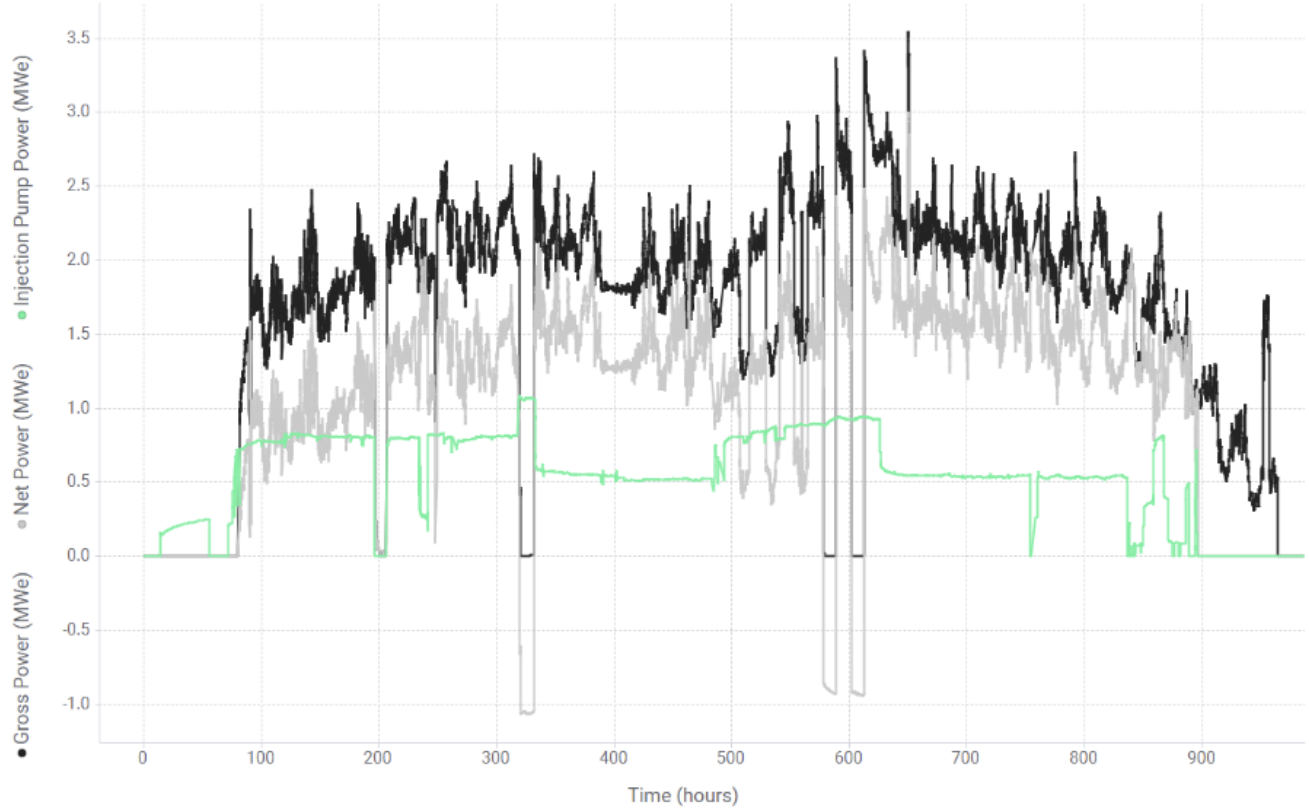

Fig. 5 Electric power production (gross and net) and injection pump power consumption during the 37-day circulation test.

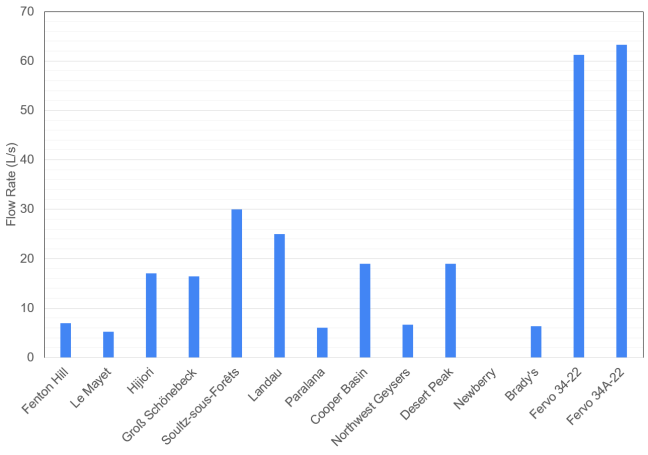

Fig. 6 Comparison of flow rate performance for historic EGS projects.

sign and multistage stimulation treatments with proppant has resulted in the most productive EGS system to-date.

3 Drilling Performance

The drilling sequence in the project was to first drill the vertical Monitoring Well 73-22, then drill Injection Well 34A-22, followed by drilling Production Well 34-22. Production Well 34-22 was drilled after the reservoir stimulation treatment was performed in Injection Well 34A-22, and the well path was planned to intersect the stimulated reservoir volume.

The days-versus depth-curves for the three wells are shown in Fig. 7. Monitoring Well 73-22 was drilled to a total depth of 8,009 ft MD in 41 days. Injection Well 34A-22 was drilled to a total depth of 11,220 ft MD in 72 days. Production Well 34-22 was drilled to a total depth of 11,211 ft MD in 59 days. We were able to achieve significant improvements in drilling performance throughout the program, resulting in an 18% reduction in total drilling days between the first and second horizontal wells. Static temperature profiles were measured with the distributed temperature sensing (DTS) fiber optic cables and calibrated against the downhole temperature gauge in 73-22 as well as wireline temperature surveys. The equilibrated temperature profiles for the three wells are shown in Fig. 8. The maximum recorded downhole temperature was 376 °F (191 °C). While there is significant opportunity to continue to improve drilling performance of horizontal geothermal wells, the performance achieved in Fervo's three well drilling campaign at Blue Mountain – in which an 18% well-over-well reduction in drilling days was achieved – validates that no barriers exist to drilling horizontal wells today and demonstrates a clear cost reduction trajectory.

4 Stimulation Treatment Design and Performance

The two horizontal wells were each completed with a plug-and-perforate (plug-and-perf) stimulation treatment design. The plug-and-perf method is currently the most commonly applied multistage stimulation method used in the unconventional oil and gas industry, as it has been proven to be a cost-effective method for improving the speed and efficiency of stimulation operations while also ensuring effective fracture initiation and prop-

Table 1 Comparison of peak flow rate measured during long-term flow rate tests following the stimulation treatment phase for several notable EGS projects throughout the world.

Project Name	Year	Flow Rate (L/s)	Reference
Le Mayet	1978	5	(Cornet 2021)
Hijiori	1988	17	(Sasaki 1998)
Fenton Hill	1992	7	(Brown et al. 2012)
Gros Schonebeck	2003	16	(Blocher and Reinsch 2015)
Paralana	2005	6	(Breede et al. 2013)
Landau	2007	25	(Schindler, Baumgartner, and Gandy 2010)
Northwest Geysers	2011	7	(Garcia, Walters, and Beall 2012)
Cooper Basin	2012	19	(Hogarth and Holl 2017)
Desert Peak	2013	19	(Akerley, Robertson-Tait, and Zemach 2020)
Bradys	2013	6	(Akerley, Robertson-Tait, and Zemach 2020)
Newberry	2014	-	(Sonnenthal, Smith, and Cladouhos 2015)
Soultz-sous-Forets	2017	30	(Baujard, Genter, and Cuenot 2018)
Fervo 34-22	2023	61	This study.
Fervo 34A-22	2023	63	This study.

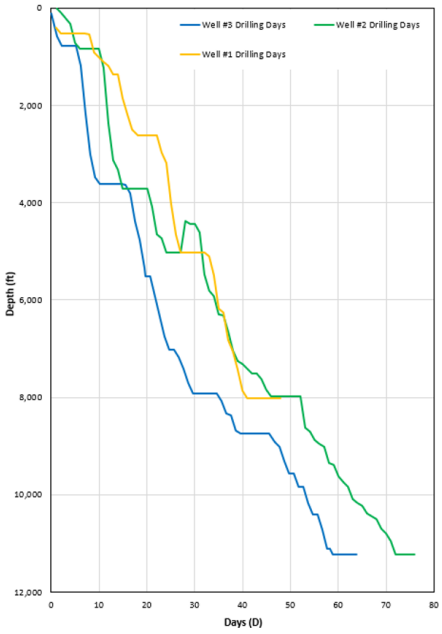

Fig. 7 Drilling performance results for Fervo's three-well drilling program at Blue Mountain. A 13-day reduction in drilling days was achieved between the first and second horizontal wells.

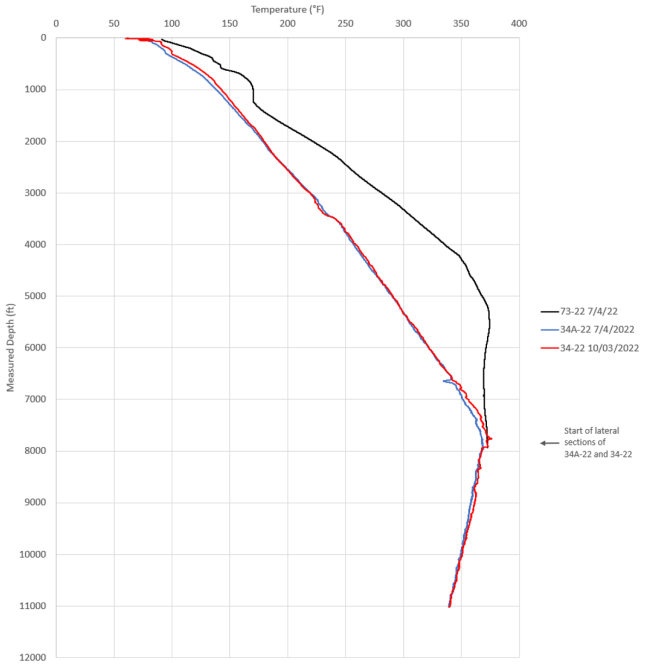

Fig. 8 Equilibrated temperature profiles for Wells 73-22, 34A-22, and 34-22. The maximum recorded temperature on the three wells was 376 °F. Although the lateral sections on 34A-22 and 34-22 are at a constant true vertical depth, the temperature tends to decline slightly towards the toe due to the temperature distribution in the project area.

Injector Well 34A-22 Pump Schedule

Stage No.	Stage Name	Pump Rate (bbl/min)	Fluid Type	Clean Volume (bbl)	Well Head Prop Conc. (ppg)	Stage Prop (lbs.)	Stage Time (min)
1	Injection	10	Slickwater	95	0	0	10
2	Acidize	10	15% HCL	24	0	0	2
3	Displacement/Pad	100	Slickwater	1,071	0	0	11
4	100 mesh	100	Slickwater	1,429	0.25	15,000	14
5	100 mesh	100	Slickwater	1,429	0.5	30,000	14
6	100 mesh	100	Slickwater	1,429	1	60,000	14
7	100 mesh	100	Slickwater	1,310	1.25	68,750	13
8	100 mesh	100	Slickwater	1,310	1.35	74,250	13
9	100 mesh	100	Slickwater	1,248	1.45	76,002	12
10	Spacer	100	Slickwater	1,000	0	0	10
11	40/70 mesh	100	Slickwater	1,310	0.75	41,250	13
12	40/70 mesh	100	Slickwater	1,310	1	55,000	13
13	40/70 mesh	100	Slickwater	1,071	1.25	56,250	11
14	40/70 mesh	100	Slickwater	1,081	1.4	63,560	11
15	Flush + 70 bbls	100	Slickwater	553	0	0	6
Total with Flush				**15,668**		**540,062**	**167**

Fluid Loading (bbl/cluster)	2,611
Proppant Loading (lb/cluster)	90,010
Fluid Loading (bbl/ft)	87
Proppant Loading (lb/ft)	2,984
Total Proppant per Stage (lbs)	540,062
Total Fluid (bbl/stage)	15,668
Clusters per Stage (-)	6

Total Proppant	540 klbs
100 mesh	324 klbs
40/70	216 klbs

Fig. 9 The stimulation treatment pumping schedule for a typical stage at Injection Well 34A-22. The stimulation treatment design was a plug-and-perforate style treatment with a low-concentration friction reducer slickwater fluid system. A combination of 40/70 mesh and 100 mesh silica proppant was used. Injection Well 34A-22 was completed with a total of 16 stages, and Production well 34-22 was completed with a total of 20 stages.

pant placement. In the plug-and-perf method, the horizontal section of a well is stimulated in stages starting at the toe of the well and sequentially moving uphole toward the heel of the well. The stage length is typically on the order of 100 ft to 300 ft, and within each stage several discrete zones along the wellbore are perforated. The stimulation involves pumping a slurry of fluid and proppant down the wellbore and through the perforations in order to initiate fractures in the rock. The proppant acts to hold the fractures open in increase their conductivity. The plug-and-perf method relies on a technique called limited entry, taking advantage of the pressure drop that occurs as fluid flow through perforations in the wellbore which then serves to passively redistribute the flow more uniformly across multiple perforation clusters located along a subsection of the horizontal well.

Injection Well 34A-22 was drilled and stimulated first. The stimulation treatment was performed over a six-day period from July 21 to July 26, 2022. A total of 16 stages were stimulated along the lateral. Each stage had roughly the same length of approximately 150 ft. All stages were planned with a similar perforation cluster design, with 6 clusters per stage and 6 perforation shots per cluster, except for Stages 12 and 13, which each had 9 clusters per stage and variable shots per cluster. The perforation clusters were designed with a limited entry style design (Gradl 2018; Weijers et al. 2019), targeting approximately 1,500 psi of perforation friction.

The treatment design called for pumping a total of approximately 16,000 bbl of fluid and 540,000 lbs of proppant in each stage. The target injection rate was 100 bpm. The stimulation fluid was a slickwater treatment design with a low-concentration friction reducer additive. The proppant was a mixture of 100 mesh and 40/70 mesh silica sand, pumped at concentrations ranging from 0.25 to 1.5 ppg. Each stage lasted approximately 3 hours. The pumping schedule for a typical stage is shown in Fig. 9.

4.1 Stimulation Effectiveness Using In-Well Fiber Optic Sensing Diagnostics

The treatment plot for a typical stage (Stage 6 on Injection Well 34A-22) is shown in Fig. 10. The in-well fiber optics data enabled us to observe key downhole behavior in real-time before, during, and after each stage. This fiber optic data provides useful information on the stimulation treatment effectiveness and the downhole conditions that various tools are exposed to.

The in-well DAS data was used to verify whether fracture initiation occurred at each perforation cluster as well as the flow allocation across all clusters in the stage. In this example, we observed that all six perforation clusters broke down and received flow for the full duration of the stage. Taking the DAS amplitude signal as a proxy for flow rate at each perforation cluster, we observed that clusters 2, 3, and 5 were the most active (see Fig. 11), however all clusters accepted fluid and the overall flow uniformity index was calculated as 73%.

During the stimulation treatment, the DTS data can be used to understand stage isolation and to determine if any leakage is occurring into the previous stage, either around the plug or behind the casing. In this example, some cooling was observed downstream of the plug in the first half of the stage, but toward the middle of the stage a clear warmback signal is observed. We attribute the relatively small amount of cooling early in the stage to most likely be caused by near-well fracture communication as fracture initiation occurred, as opposed to a leaky plug. The relatively low levels of acoustic activity downstream of the bridge plug indicate that good stage isolation was achieved.

We were able to record in-well fiber optic sensing data for 13 out of the 16 stages in Injection Well 34A-22. Upon analyzing the fiber data for all stages, we found that fracture breakdown and initiation occurred at 100% of the perforation clusters, regardless of the lithology that the perforation clusters were located in. The uniformity index ranged from 56% to 81% across all stages (see Fig. 12). The stages with nine clusters also showed relatively good flow distribution, verifying that extreme limited entry completions are likely a viable path towards meaningful cost reductions in future drilling campaigns (Weijers et al. 2019; Somanchi, Brewer, and Reynolds 2018). In addition, we found no evidence of any bridge plug failures, indicating that the bridge plugs used in this project were rated to sufficient temperature and differential pressure ratings for the downhole conditions that were experienced.

5 Reservoir Characterization

The economics of EGS projects are driven by a combination of engineering design choices (e.g., target well depth, lateral length, and stimulation treatment volumes) as well as reservoir performance characteristics that are largely influenced by geological factors (e.g., fracture conductivity, total fracture surface area, and well connectivity). We designed a comprehensive data acquisition campaign to evaluate key reservoir properties that have a primary control on system performance. Here, we describe key data and observations that enabled us to characterize the geometry of the stimulated reservoir volume and flow capacity of the system.

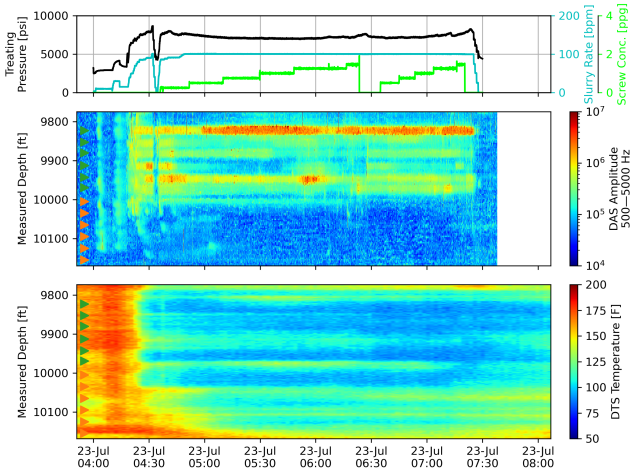

Fig. 10 Treatment plot showing surface injection pressure, injection rate, and proppant concentration (top); DAS waterfall plot showing acoustic signal and location of the perforation clusters from the active stage and previous stage (middle); DTS waterfall plot showing the temperature variations along the well throughout the duration of the active stage (bottom).

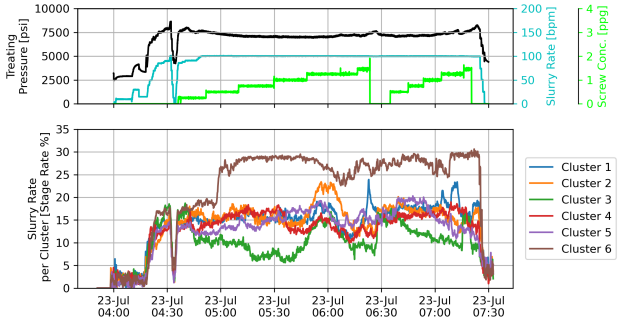

Fig. 11 Treatment plot for a typical stage (top) and DAS-derived slurry rate allocation for each of the six perforation clusters in the treatment stage (bottom). The target total slurry injection rate during that stage was 100 bpm, corresponding to a target of 16.7 bpm per cluster. The cluster-level flow allocation shows that 4 out of 6 clusters received the target flow rate and the remainder of the flow as spread across the other two clusters.

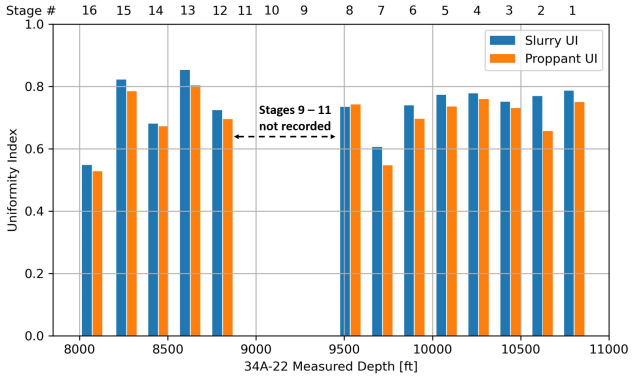

Fig. 12 Flow uniformity index for both fluid and slurry based on correlations with DAS data for 13 out of 16 stages from Well 34A-22. The flow uniformity indices range from 56% to 81% across all stages monitored, with the majority of stages exhibiting slurry uniformity indices greater than 70%.

5.1 Stimulated Reservoir Volume

The purpose of the multistage, multicluster stimulation treatment program is to enhance the permeability of the reservoir, create extensive fracture surface area the enable sustainable heat transfer rates, and distribute flow uniformly throughout the reservoir to improve thermal recovery factors. The geometry of the stimulated reservoir volume (SRV) is a useful metric for characterizing reservoir performance. Here, we describe how we use a variety of independent datasets to constrain the SRV geometry, including microseismic monitoring, strain monitoring using low-frequency distributed acoustic sensing fiber optics, and reservoir pressure monitoring using permanent bottomhole pressure gauges in offset wells.

The stimulation of Injection Well 34A-22 and Production Well 34-22 produced a significant number of microseismic events which were able to be detected with a favorable signal-to-noise ratio on multiple permanent fiber optic cables. The highest quality events from both treatments are shown in Fig. 13.

The merged data from the vertical and horizontal fibers significantly improves the confidence of the event locations. However, the measurements of axial strain along the fibers imply that there is inherent uncertainty in the event location, particularly in the horizontal directions. Nonetheless, the distribution of the microseismic events provide information on the extent and geometry of the SRV.

Figure 14 shows the distribution of microseismic events away from the horizontal doublet and with depth. To get the distribution shown on the left, we rotated microseismic clouds to 10 degrees to the north, accounting for the well azimuth, and stacked the events for all stages. The zero point corresponds to the middle in between 34A-22 and 34-22, the locations of which are indicated with dash-dotted lines. For the right plot, we directly used events depth. We calculated the total number of observed high-quality events in the bins of 100 ft. To define SRV boundaries, we selected the bins which have more than 100 events for either of the stimulation treatments. Microseismic-derived SRV length is 2,300 ft and height of 2,500 ft. Low-frequency indicates that the half-length is more than 800 ft, and the top half-height of 400 ft

from the middle point between the injector and producer.

5.2 Reservoir Flow Characteristics

The horizontal well EGS concept developed in this project is designed to enhance the reservoir permeability during the stimulation treatment phase by creating a distributed network of fractures along the wellbores. Fracture propagation occurs during the stimulation phase and acts to connect the wells hydraulically, and proppant that is pumped with the treatment fluid ultimately acts to preserve the fracture conductivity throughout the subsequent production phase. Prior to this project, a multistage, multicluster stimulation treatment with proppant had not been performed in a mixed metasedimentary and igneous formation. Limited data exists on stimulated reservoir permeability and propped fracture conductivity in this geologic setting, therefore the crossflow production test was designed to enable characterization of these key reservoir properties.

For a horizontal well doublet system connected by a set of uniform vertical fractures, flow in the fractured reservoir system between the wells can be characterized using Darcy's Law as:

$$q = \frac{kA}{\mu}\frac{\Delta p}{\Delta L}, \tag{5}$$

where q is volumetric flow rate, k is the permeability of the fractures, A is the total cross-sectional area of the fracture system, μ is reservoir fluid viscosity, Δp is pressure drop across the reservoir (i.e., the difference in bottomhole pressure between the injection and production well), and ΔL is the offset spacing between the wells. Assuming that the wells are connected by a set of n vertical fractures, each with fixed height h and aperture w, Eq. 5 can be rewritten in terms of the fracture properties as:

$$q = \frac{nkwh}{\mu}\frac{\Delta p}{\Delta L}. \tag{6}$$

In Eq. 6, we can define the fracture conductivity as $c = kw$. In addition, we can define the overall reservoir transmissibility as:

$$\Upsilon \equiv \frac{q}{\Delta p} = \frac{nkwh}{\mu \Delta L}, \tag{7}$$

which is a measure of the overall flow capacity of the system. Equations 5 – 7 assume that the matrix permeability is negligible and that flow occurs primarily through the fractures.

Phase 1 of the crossflow test was designed as a pressure interference test in which fluid was injected into Injection Well 34A-22 at a constant rate of approximately 10 bpm while Production Well 34-22 and Monitoring Well 73-22 were maintained in a shut-in condition. The pressure transients were observed at all three wells during the constant-rate injection period. After 42 hours of injection, Injection Well 34A-22 was shut-in and pressure falloff was monitored at all wells.

Prior to starting the test, both wells were in static conditions. The reservoir fluid, initial wellbore fluid, and injectate were similar fluids, which can be classified as low-salinity brine with total dissolved solids (TDS) levels below 5000 ppm and non-condensible gas (NCG) content below 0.5% weight fraction. Therefore, we assume fluid properties to be similar to freshwater. Based on static temperature profiles measured along the laterals of both horizontal wells as well as a bottomhole temperature gauge installed in Monitoring Well 73-22, the average initial reservoir temperature is estimated to be 363 °F.

We observed a nearly instantaneous pressure response at the offset wells, indicating a highly permeable fractured reservoir system. After approximately 5 to 10 hours of constant-rate injection, we observed that pseudo-steady-state pressure transient behavior was established. A fixed pressure differential between Injection Well 34A-22 and Production Well 34-22 of approximately 205 psi was observed consistently throughout the test period. This behavior allowed us to evaluate the reservoir transmissibility and the propped fracture conductivity for the horizontal well EGS system.

Pressure throughout the Phase 1 constant-rate injection test was measured at the injector and producer wellheads. The test was performed at a relatively low flow rate of 10 bpm. Injection temperatures varied between 75 to 125 °F. We monitored the downhole temperature profile along Injection Well 34A-22 continuously using DTS measurements, giving us accurate downhole fluid temperature measurements throughout the test. We estimated the frictional pressure drop while injecting fluid through 7" casing (150 °F bottomhole temperature) to be approximately 55 psi using standard assumptions for pipe flow, which allowed us to correct for bottomhole pressure at Injection Well 34A-22. Production Well 34-22 was shut-in during the entire test, and therefore the wellhead pressure change is approximately equal to the bottomhole reservoir pressure change (i.e., there was no frictional pressure drop in the production well during this test).

In the plug-and-perf stimulation treatment designed used in this project, it is assumed that a single fracture zone initiates at each perforation cluster. Following the stimulation treatment program, total of 102 perforation clusters were created along Injection Well 34-22 at an average spacing of 30 ft, and 94 perforation clusters were created along Production Well 34-22 also at an average spacing of 30 ft. In-well distributed fiber optic sensing measurements recorded during the 34A-22 stimulation treatment suggested that fracture initiation occurred at 100% of the perforation clusters with an average flow uniformity index of about 70%.

Several wireline spinner surveys were performed in Injection Well 34A-22 during Phase 7 of the crossflow test to measure the flow distribution along the lateral. In Fig. 15, we show the flow distribution while injecting at 12.5 bpm, similar to the injection rate during Phase 1 of the test. We observed that although the flow was not perfectly uniform, fluid flow was distributed along the entire lateral. We did not observe significant heel bias (i.e., flow predominantly exiting the wellbore within the heel-most stages of the lateral). Similarly, there were no indications that flow localized into a small subset of zones, confirming that the stimulation treatment design did not result in significant fast flowing pathways that could lead to thermal short-circuiting during long-term operations. Based on the combination of the flow allocation measurements recorded using distributed fiber optic sensing during the stimulation treatment and the flow profile surveys recorded during the crossflow test, most fracture zones along the

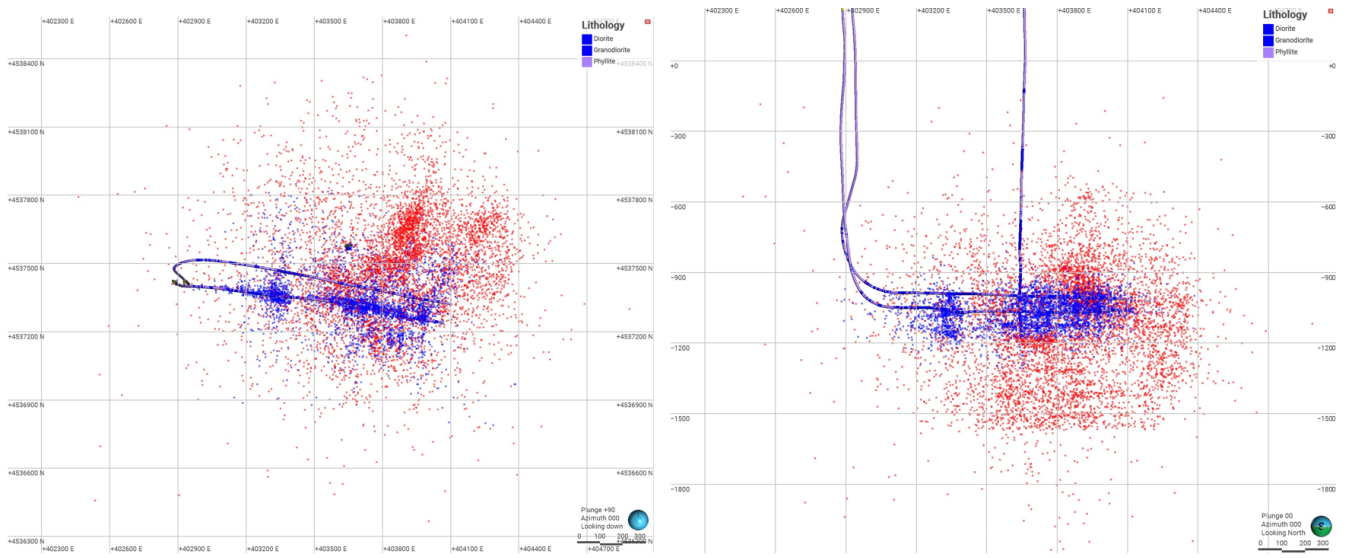

Fig. 13 Plan view (left) and cross-section view (right) of the distribution of microseismic events recorded during the stimulation treatments of Injection Well 34A-22 (blue dots) and Production Well 34-22 (red dots). These events represent the locations of the highest quality events detected on the multiwell DAS fiber optic sensing array.

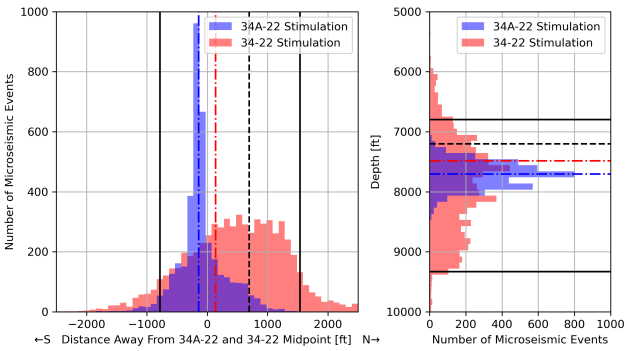

Fig. 14 Microseismic-derived stimulated reservoir volume geometry. Histograms indicate microseismic events distributions away from the wells (left) and with depth (right) for both 34A-22 and 34-22 stimulation treatments. The reference locations of the wells are indicated with dash-dotted lines. The solid lines represent the interpreted extent of the induced fractures.

lateral actively contribute conductivity to the EGS system.

The bottomhole pressure differential while flowing at $q = 10$ bpm was calculated as $\Delta p = 151$ psi .The average offset spacing between Injection Well 34A-22 and Production Well 34-22 was $\Delta L = 365$ ft as calculated from the wellbore surveys. The effective fracture height was assumed to be $h = 300$ ft, which is a conservative fraction of the SRV fracture height interpreted from low-frequency DAS and microseismic monitoring. The reservoir fluid viscosity was assumed to be $\mu = 0.3$ cp based on an average between the initial reservoir temperature (363 °F) and the injected fluid temperature at bottomhole conditions (approximately 150 °F). The total number of active fracture pathways is assumed to range from $n = 75$ to $n = 100$ to account for uncertainty on the flow distribution along the wellbores and connectivity throughout the reservoir. A summary of the key reservoir and fluid properties used in the analysis are listed in Table 2.

Based on these data and measurements, we are able to estimate the total reservoir transmissibility of the horizontal EGS system as well as the effective propped fracture conductivity. We found that the reservoir transmissibility was $\Upsilon = 0.07$ bpm per psi (25.5 L/s per MPa). Depending on the assumed number of flowing fracture pathways, this transmissibility equates to an individual fracture conductivity of 300 md·ft to 400 md·ft (9.1×10^{-14} m^3 to 1.2×10^{-13} m^3).

The reservoir transmissibility and fracture conductivity measurements are encouraging from the perspective of operating the system under long-term production operations as well as in extrapolating performance under future EGS system designs. Under commercial operating conditions, we anticipate circulating 20 bpm to 30 bpm through the system. This suggests that we can expect about 300 to 450 psi of pressure drop across the reservoir, which is manageable with standard injection pump and artificial lift equipment. In future EGS designs, we anticipate extending the lateral length up to 5000 ft to 7500 ft. Reservoir transmissibility scales linearly with lateral length and the number of fracture zones (Shiozawa and McClure 2014), therefore by increasing the lateral length it should be possible to reduce the pressure drive across the reservoir, enable wider offset well spacing, or enable significantly higher flow rates, each of which would dramatically improve the system performance.

Compared to the most well-characterized historic EGS project, Soultz-sous-Forets, our horizontal, multistage well design resulted in significantly higher reservoir transmissibility. At Soultz, the effective reservoir transmissibility was about 0.01 bpm per psi (3.7 L/s per MPa), about a factor of 7 lower (Shiozawa and McClure 2014). Similarly, the fracture conductivity values measured in our horizontal EGS system (300 md·ft to 400 md·ft) are generally higher than is typically found in field data from unconventional shale projects. For example, Mouin et al. 2023 used inter-

ference testing on unconventional shale wells from the Delaware basin and found that fracture conductivity ranged from 10 to 135 md·ft. This suggests that perhaps the conductivity of propped fractures in metamorphic or igneous rocks may be higher than for shales.

Table 2 Properties used to evaluate reservoir transmissibility and fracture conductivity.

Parameter	Value	Unit
q	10	bpm
h	300	ft
μ	0.3	cp
Δp	151	psi
ΔL	365	ft
n	75 - 100	-

6 Induced Seismicity

Prior to starting the operations phase of this project, a preliminary screening assessment was performed to evaluate the potential risk of induced seismicity at the project site. We followed the guidelines outlined by the US Department of Energy's Protocol for Addressing Induced Seismicity Associated with Enhanced Geothermal Systems (Majer et al. 2012). Based on our analysis, we developed and implemented a Traffic Light System (TLS) to mitigate the risk of potential induced seismicity associated with the project. The TLS system was in effect throughout all major phases of the project from July 2020 through June 2023, including drilling, completions, stimulation, and well testing. All observed seismicity fell within the Green TLS protocol, with no significant impact or incident throughout the full duration of the project.

The project site is located adjacent to the Blue Mountain geothermal facility in Churchill County, Nevada. The nearest town is Winnemucca, located approximately 34 km (21 miles) from the project site. The Blue Mountain geothermal power plant that has been under active commercial operations since 2009 with no reported cases of induced seismicity. Based on a search of the US Geological Survey (USGS) ComCat earthquake catalog, there have been zero recorded seismic events with magnitude $M > 2$ within a 20 km (12 mile) search radius around the project area. Expanding the search radius to 40 km (25 miles), we found a total of five events ranging in magnitude between $2.1 \leq M \leq 2.8$. Therefore, we concluded that the Blue Mountain field is located in an area with minimal natural seismicity.

A local seismic monitoring network was first installed by the plant operator in 2015. In July 2020, Fervo Energy commissioned a new local seismic monitoring network consisting of 8 broadband seismometers, a local strong motion sensor installed at the power plant facility, and another strong motion sensor installed in the town of Winnemucca. The local seismic network was operated continuously from July 2020 through June 2023 in partnership with the USGS. The network provided real-time event detection and locations, and was designed to achieve a magnitude of completeness down to approximately $M = -1$.

We evaluated USGS ShakeMap data for historic natural seismicity in north-central Nevada to develop an empirical peak ground acceleration response curves for relatively large earthquakes with magnitudes ranging from $3.5 \leq M \leq 6.0$ (see Fig. 17). The USGS ShakeMap models take into account local ground motion models for the region, and therefore these data provide a good representation for how ground shaking intensity varies with distance for a range of earthquake magnitudes. We find that based on the distance of the project site to the nearest population center, earthquakes up to $M = 5$ with epicenters near the project area generally would be expected to result in weak ground motions, with Modified Mercalli Intensity (MMI) values of MMI III or lower.

Based on the understanding of ground motion response in the local area, we established a Traffic Light System (TLS) protocol that consisted of Green, Yellow, and Red thresholds. Under the Green level (events with $M < 2.0$), normal operations continue as planned. Under the Yellow level ($2.0 \leq M < 3.0$), operations are modified to mitigate the risk of triggering larger events, including reducing pumping volumes, reducing injection rates, and suspending operations. Under the Red level ($M \geq 3.0$), injection rates and pressures are reduced to zero, flowback of fluid is performed to reduced reservoir pressures, and operations are suspended until further technical review and stakeholder engagement is performed.

During periods of no active operations, we observed relatively low levels of background seismicity (on average about three to five events per week). During periods of stimulation or well testing activity, we observed that seismicity rates increased. In Fig. 18, we show the full catalog of events that were detected and located throughout the full project duration. Seismicity rates were highest during the stimulation treatment phases. The largest magnitude recorded was a $M = 1.8$ event, which occurred during the 37-day crossflow test. As shown in Fig. 18, all observed seismicity remained within the Green level throughout all phases of the project.

7 Conclusions

Fervo Energy drilled, completed, and tested a first-of-a-kind enhanced geothermal system in northern Nevada. The EGS system consisted of a pair of horizontal geothermal wells, and the reservoir permeability was enhanced using the plug-and-perforate stimulation treatment method. The stimulation treatment resulted in creating over 100 discrete fracture zones that served to connect the two horizontal wells hydraulically and provided heat transfer surface area required to recover thermal energy from the formation. We performed a long-term production performance test by circulating fluid from the injection well to the production well at commercially relevant operating conditions over a 37-day period.

We demonstrated that the horizontal EGS system is capable of achieving flow rates of up to 63 L/s, equivalent to a peak gross electric power output of 3.5 MW. The flow rate and power output achieved in the crossflow production test exceed the performance measured at other historic EGS projects.

The distribution of fluid flow along the lateral was characterized during steady-state production using a wireline spinner survey. The flow distribution was observed to be relatively uniform, with flow actively occurring the entire lateral and no significant

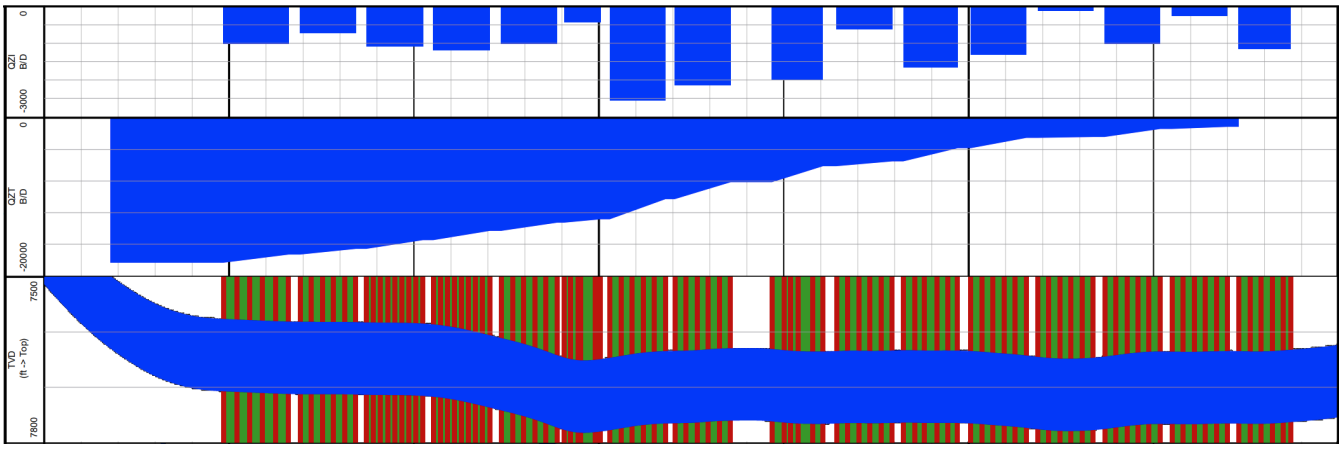

Fig. 15 Injection flow profile spinner log survey recorded in Injection Well 34A-22 during the crossflow test. The flow profile image shows stage level injection rate allocation (top), a continuous record of total flow along the lateral (middle), and the lateral geometry and location of all perforation clusters along the lateral (bottom). The flow profile was measured using a spinner log that was tractored along the lateral while injecting at a flow rate of 12.5 bpm.

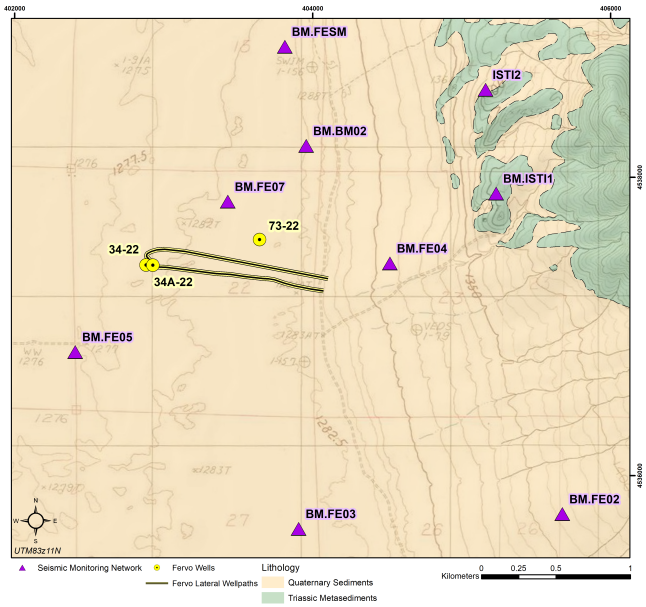

Fig. 16 Site map of the project area highlighting the location of the shallow borehole seismic monitoring array. The array consists of 8 broadband seismommeters capable of recording and telemetering real-time measurements. In addition, the seismic monitoring network consists of two strong motion accelerometers, one located at the power plant (labeled BM.FESM) and another located in the town of Winnemucca (not shown on map).

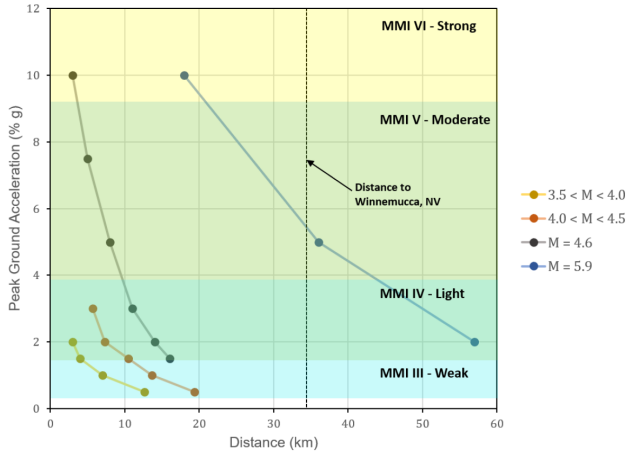

Fig. 17 Empirically-derived ground motion model for the project area.

localized flow pathways. Production fluid temperature continually increased throughout the crossflow test, indicating that no severe thermal short-circuit pathways were created during the stimulation treatment. For the full duration of the crossflow test, flow rates through the system were driven entirely by surface injection pumps, confirming that the EGS system behaved as a confined system. Artificial lift was not required to sustain flow rates in the production well.

A major focus of the project was on executing a comprehensive data acquisition program, which included diagnostic fracture injection tests, downhole microseismic monitoring, in-well and cross well distributed fiber optic sensing, and reservoir pressure monitoring with downhole gauges. The combination of multiple independent datasets provided detailed insight into the downhole conditions during the stimulation treatment as well as a well-characterized understanding of the stimulated reservoir volume geometry and other properties that impact reservoir performance of the doublet well system. We found that the stimulated reservoir volume geometry could be characterized as approximately

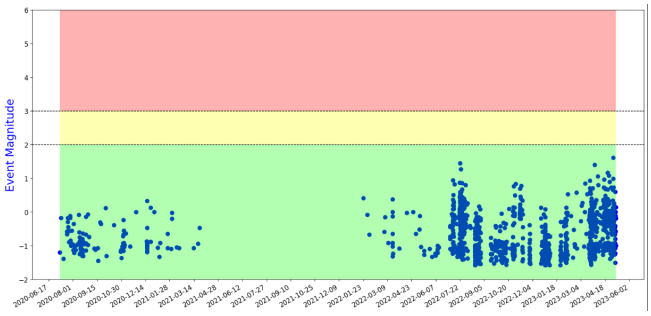

Fig. 18 Seismic event catalog recorded by the local seismic monitoring array over the period of July 2020 through June 2023, covering all major phases of the project including drilling, completions, stimulation, and well testing. All observed seismicity remained under the Green level in the Traffic Light System, with no incidents or impacts throughout the entire duration of the project.

3000 ft along the lateral length, 1600 ft to 2,300 ft perpendicular to the wells, and 800 ft to 2,500 ft high. We observed fracture initiation at 100% of the perforation clusters monitored with in-well distributed acoustic sensing. The stimulated reservoir volume geometry and stimulation effectiveness support economic levels of heat recovery for the system. Based on pressure transient analysis, we estimated the conductivity of propped fractures in the system to range from 300 to 400 md·ft.

Having successfully completed the drilling, completion, and well construction phase of the project, we have demonstrated that currently no technical barriers exist to developing horizontal well geothermal drilling programs in high-temperature, hard rock settings. The project was completed using drilling and completions tools and technology that already commonly exist in the industry. Reservoir simulation forecasts and history matching were able to replicate key reservoir response observations, indicating that physics-based modeling can effectively be used to evaluate reservoir performance of horizontal well geothermal systems.

Acknowledgements

This work was partially funded by the US Department of Energy and the University of Utah through the following awards: Award Nos. DE-AR001153, DE-AR0001604, and DE-EE0008486. In addition, partial funding was provided by DOE EERE Geothermal Technologies Office to Utah FORGE and the University of Utah under Project DE-EE0007080 Enhanced Geothermal System Concept Testing and Development at the Milford City, Utah Frontier Observatory for Research in Geothermal Energy (Utah FORGE) site.

References

Akerley, J.H., A. Robertson-Tait, and E. Zemach. 2020. “Near-field EGS: A review and comparison of the EGS demonstration projects at Desert Peak and Bradys.” World Geothermal Congress, Reykjavik, Iceland.

Augustine, C., S. Fisher, J. Ho, I. Warren, and E. Witter. 2022. *Enhanced Geothermal Shot Analysis for the Geothermal Technologies Office.* Technical report NREL/TP-5700-84822. National Renewable Energy Laboratory.

Baujard, C., A. Genter, and N. Cuenot. 2018. “Experience learnt from a successful soft stimulation and operational feedback after 2 years of geothermal power and heat production in Rittershoffen and Soultz-sou-Forets plants (Alsace, France).” Geothermal Resources Council Transactions.

Beckers, K.F., and K. McCabe. 2019. “GEOPHIRES v2.0: Updated geothermal techno-economic simulation tool.” *Geothermal Energy* 7 (5).

Blocher, G., and H. Reinsch. 2015. “Hydraulic history and curent state of the deep geothermal reservoir Groß Schönebeck.” *Geothermics* 63:27–43.

Breede, K., K. Dzebisashvili, X. Liu, and G. Falcone. 2013. “A systematic review of enhanced (or engineered) geothermal systems: past, present and future.” *Geothermal Energy* 1 (4): 1–27.

Brown, D., D. Duchange, G. Heiken, and V. Hriscu. 2012. *Mining the Earth’s Heat: Hot Dry Rock Geothermal Energy.* Springer.

Cornet, F.H. 2021. “The engineering of safe hydraulic stimulations for EGS development in hot crystalline rock masses.” *Geomechanics for Energy and the Environment* 26 (100151).

DOE. 2019. *GeoVision: Harnessing the Heat Beneath our Feet.* Technical report. U.S. Department of Energy (DOE).

Faulds, J., and N.H. Hinz. 2016. “Favorable tectonic and structural settings of geothermal settings in the Great Basin Region, western USA: Proxies for discovering blind geothermal systems.” World Geothermal Congress, Melbourne, Australia.

Garcia, J., M. Walters, and J. Beall. 2012. “Overview of the Northwest Geysers EGS demonstration project.” 37th Workshop on Geothermal Reservoir Engineering, Stanford, California, USA.

Gradl, C. 2018. “Review of recent unconventional completions innovations and their applicability to EGS wells.” 43rd Workshop on Geothermal Reservoir Engineering, Stanford, California, USA.

Hogarth, R., and H. Holl. 2017. “Lessons learned from the Habanero EGS project.” Geothermal Resources Council Transactions.

Latimer, T., and P. Meier. 2017. “Use of the experience curve to understand economics for at-scale EGS projects.” 42nd Workshop on Geothermal Reservoir Engineering, Stanford, California, USA.

Majer, E., J. Nelson, A. Robertson-Tait, J. Savy, and I. Wong. 2012. *Protocol for addressing induced seismicity associated with Enhanced Geothermal Systems.* Technical report. US Department of Energy Geothermal Technologies Office, number=DOE/EE-0662.

McClure, M.W., and R.N. Horne. 2014. “An investigation of stimulation mechanisms in Enhanced Geothermal Systems.” *International Journal of Rock Mechanics and Mining Sciences* 72:242–260.

Mouin, A., T. Andrews, C. Johnston, A. Singh, and M. McClure. 2023. “A new method for interpreting well-to-well interference tests and quantifying the magnitude of production impact: theory and applications in a multi-basin case study.” *Geomechanics and Geophysics for Geo-Energy and Geo-Resources* 9 (95).

Norbeck, J.H., M.W. McClure, and R.N. Horne. 2018. “Field observations at the Fenton Hill enhanced geothermal system test site support mixed-mechanism stimulation.” *Geothermics* 74:135–149.

NREL. 2023. *2023 Annual Technology Baseline.* Technical report. Golden, CO: NREL (National Renewable Energy Laboratory).

Ricks, Wilson, Jack Norbeck, and Jesse Jenkins. 2022. “The value of in-reservoir energy storage for flexible dispatch of geothermal power.” *Applied Energy* 313:118807. ISSN: 0306-2619. https://doi.org/https://doi.org/10.1016/j.apenergy.2022.118807.

Sasaki, S. 1998. “Characteristics of microseismic events induced during hydraulic fracturing experiments at the Hijiori hod dry rock geothermal energy site, Yamagata, Japan.” *Tectonophysics* 289:171–188.

Schindler, M., J. Baumgartner, and T. Gandy. 2010. “Successful hydraulic stimulation techniques for electric power production in the Upper Rhine Graben, Central Europe.” World Geothermal Congress, Bali, Indonesia.

Sepulveda, N.A., J.D. Jenkins, F.J. de Sisternes, and R.K. Lester. 2018. “The Role of Firm Low-Carbon Electricity Resources in Deep Decarbonization of Power Generation” [in English (US)]. *Joule* 2 (11): 2403–2420. ISSN: 2542-4351. https://doi.org/10.1016/j.joule.2018.08.006.

Shiozawa, S., and M. McClure. 2014. “EGS designs with horizontal wells, multiple stages, and proppant.” 39th Workshop on Geothermal Reservoir Engineering, Stanford, California, USA.

Somanchi, K., J. Brewer, and A. Reynolds. 2018. “Extreme limited-entry design improves distribution efficiency in plug-and-perforate completions: Insights from fiber-optic diagnostics.” *SPE Drilling and Completions* 33 (04): 298–306.

Sonnenthal, E., J. Smith, and T. Cladouhos. 2015. “Thermal-hydrological-mechanical-chemical modeling of the 2014 EGS stimulation experiment at Newberry Volcano, Oregon.” 40th Workshop on Geothermal Reservoir Engineering, Stanford, California, USA.

Weijers, L., C. Wright, M. Mayerhofer, M. Pearson, L. Griffin, and P. Weddle. 2019. “Trends in the North American frac industry: Invention through shale revolution.” Paper SPE 194345-MW, SPE Hydraulic Fracturing Technology Conference, The Woodlands, Texas, USA.